Journal of proteome research

Open Access

pubs.acs.org/jpr

Article

Upregulations of SNAT2 and GLS-1 Are Key Osmoregulatory Responses of Human Corneal Epithelial Cells to Hyperosmotic Stress

Kenrick Kai-yuen Chan,[⊥] Alan Chun-kit Lee,[⊥] Shing-yan Roy Chung, Man-sau Wong, Chi-wai Do, Thomas Chuen Lam, and Hang-Kin Kong*

Cite This: *J. Proteome Res.* 2025, 24, 2771−2782

Read Online

ACCESS | Metrics & More | Article Recommendations | Supporting Information

ABSTRACT: Dry eye syndrome (DES) affects millions of people worldwide. However, as the cellular responses of the corneal epithelium under hyperosmotic stress remain unclear, this study investigated the proteomic changes between human corneal epithelial cells (HCECs) cultured with isosmotic and hyperosmotic media. Under hyperosmotic stress, HCECs increased expressions of sodium-coupled neutral amino acid transporter (SNAT2), glutaminase (GLS-1), and a few isoforms of heat shock protein and aldo-keto reductase family 1. The expressions of SNAT2 and GLS-1 were increased after 6 h of exposure to hyperosmotic stress but not by glutamine deprivation. The hyperosmotic stress increased intracellular levels of glutamine, mitochondrial superoxide, and mitochondrial membrane potential and induced mitochondrial fission in HCECs. Thus, the intracellular level of glutamine was elevated in the hyperosmotic stressed HCECs via the upregulation of SNAT2. Glutamine can act as an osmolyte to regulate the osmolarity of HCECs or be converted to glutamate by GLS-1 for the tricarboxylic acid cycle and oxidative phosphorylation to maintain ATP production under the hyperosmotic stress-induced mitochondrial fission. Thus, the increases in the expressions of SNAT2 and GLS-1 are key osmoregulations in HCECs upon the hyperosmotic stress and may act as corneal biomarkers for monitoring DES progression.

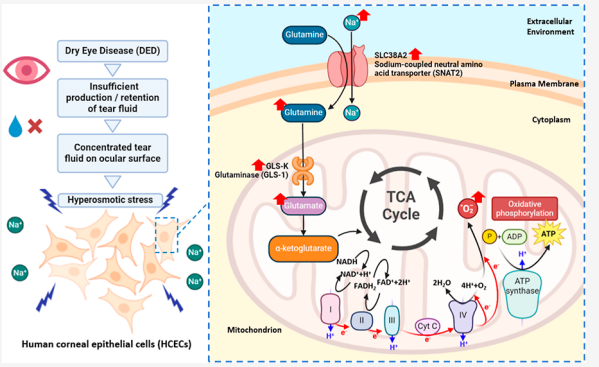

KEYWORDS: *dry eye syndrome, corneal epithelial cell, sodium-coupled neutral amino acid transporter (SNAT2), glutaminase (GLS-1), glutamine, mitochondria*

1. INTRODUCTION

Dry eye syndrome (DES) is one of the most common ocular surface diseases with an estimated global prevalence of about 11%.[1] DES is characterized by the loss of tear film homeostasis, resulting in tear film instability and hyperosmolarity, subsequently inducing inflammation and causing damage to the ocular surface.[2] Dysfunction of the meibomian glands is one of the leading causes of evaporative DES.[3] Patients who suffer from DES experience various discomforts, including dryness, itchiness, and a burning sensation, which significantly impact their quality of life.[4,5] Due to the instability of the tear film, the corneal epithelium is highly susceptible to hyperosmolarity, leading to inflammation and apoptosis.[6−12] In the absence of sufficient tear lubrication over an extended period, the corneal epithelium is at an increased risk of abrasion and erosion, potentially resulting in an uneven thickness of the corneal layer.[13,14]

In addition to the corneal epithelium, various other tissues and cell types are also susceptible to hyperosmotic conditions, either naturally or due to various diseases, and cell-type-specific responses may be exhibited by different types of epithelial cells. Due to countercurrent multiplication, the renal medulla is naturally exposed to elevated osmolarity. The cellular responses and the proteomic changes of the renal medulla may elucidate its osmoadaptation in the hyperosmotic environment. An in vitro study on murine inner medullary collecting tube 3 cells revealed that its cell cycle was arrested in the G0/G1 phase.[15] Expressions of α Crystallin B, osmotic stress protein, aldose reductase, as well as isoforms of heat shock protein 70 (HSP 70) and translation elongation factor in murine inner medullary collecting tube 3 cells were constitutively high, which may enhance their tolerance under the hyperosmotic stress.[16,17] Another study on epithelial cells of the thick ascending limb of Henle's loop reported that the expressions of aldose reductase, α Crystallin B, HSP 70, and HSP 90 were increased under the hyperosmotic conditions.[18] These studies suggest that the increase in the expression of HSP upon hyperosmotic stress may be a common cellular response

Received: November 22, 2024
Revised: March 18, 2025
Accepted: March 30, 2025
Published: May 13, 2025

https://doi.org/10.1021/acs.jproteome.4c01046
J. Proteome Res. 2025, 24, 2771−2782

among different epithelial cells. However, as the expressions of HSPs in human cells were known to be increased under various types of stresses, the increase in the HSP expression may not be considered as an osmoregulatory response in human cells.[19]

Skin is another tissue which frequently experiences local osmotic changes, especially when suffering from irritant contact dermatitis and atopic dermatitis. A few studies have investigated the effects of hyperosmotic stress on skin using various in vitro and in vivo models. Similar to the studies mentioned previously, the expression of aldose reductase was greatly increased in human embryonic epithelial cells after exposure to hyperosmotic stress.[20] A subsequent study of murine embryonic fibroblasts reported that HSP70.1 deficiency markedly reduced their viability under hyperosmotic stress compared to the wild-type fibroblasts.[21] During water loss in atopic dermatitis, sodium channel Nax was found to mediate inflammation in keratinocytes.[22] Expression of chloride channel accessory 3A2 in murine skin was reported to be increased by low humidity, which could protect the keratinocytes from apoptosis induced by the hyperosmolarity.[23] Serine protease 35 (PRSS35) was found to modulate the extracellular matrix proteome in fibroblasts under the hyperosmotic stress.[24] The findings from the skin cells revealed that other than HSP, hyperosmotic stress might elicit diverse osmoregulatory responses, like inducing the expressions of different ion channels in different epithelial cell types. Thus, it is suspected that the corneal epithelium may also exert cell-type-specific cellular responses to hyperosmotic stress.

Despite the growing interest in the impact of hyperosmotic stress on corneal epithelial cells, current research has predominantly focused on its effect on inducing apoptosis and inflammation. It has been reported that hyperosmotic pressure induced apoptosis in the human corneal epithelial cells (HCECs) through activation of Polo-like kinase 3 (Plk3) and c-jun N-terminal kinase/mitogen-activated protein kinase (JNK/MAPK) signaling pathways.[11,25,26] In addition, hyperosmotic stress also promoted inflammation via the gasdermin D (GSDMD)-dependent pyroptotic pathway[11] and activation of the NOD-, LRR-, and pyrin domain-containing protein 3 (NLRP3) inflammasome in corneal epithelial cells.[12,27] Although these studies have provided valuable insights into the clinical manifestations of DES, they offer a limited perspective on the broader molecular mechanisms underlying cellular responses to hyperosmotic conditions. To address this gap, a comprehensive proteome-wide investigation is essential. This study aimed to leverage a proteomic approach to identify novel pathways and biomarkers, followed by biological assays to characterize their functional roles, and ultimately validate these findings to establish a more comprehensive understanding of corneal epithelial cell behavior against hyperosmotic stress. Through this integrated strategy, the study aimed to reveal previously unrecognized cell-type-specific responses of human corneal epithelial cells and provide a foundation for future development of therapeutic interventions for DES.

2. MATERIALS AND METHODS

2.12.1. Human Corneal Epithelial Cell (HCEC) Culture and Induction of Hyperosmotic Stress and Depletion of Glutamine in HCEC

The human corneal epithelial cell (HCEC) was purchased from BeNa Culture Collection (#BNCC337876, BNCC, Beijing, China). HCECs were cultured with Dulbecco's modified Eagle's medium F12 (DMEM/F12; #11320033, ThermoFisher, Waltham, MA, USA) with 10% fetal bovine serum (FBS; #A5256701, ThermoFisher) and 1% penicillin−streptomycin antibiotic mixture (P/S; #15140122, ThermoFisher) at 37 °C with 95% humidity and 5% CO_2.[28] HCECs between passages 4 and 9 were used in this study. DMEM/F12 and DMEM/F12-G (glutamine-free; #21331020, ThermoFisher) were used for the preparation of hyperosmotic media. Sodium chloride was added to DMEM/F12 and DMEM/F12-G so that the osmolarities of the media were adjusted to either 312 mOsM (isosmotic) or 450 mOsM (hyperosmotic) with the aid of a laboratory osmometer (OM807 Vogel, GmbH, Kevelaer, Germany). HCECs were subjected to 4 treatments: NRM (isosmotic DMEM/F12), NRM -Gln (isosmotic DMEM/F12 without glutamine), HiOs (hyperosmotic DMEM/F12), and HiOs -Gln (hyperosmotic DMEM/F12 without glutamine) as previously reported with modifications.[29] HCECs were then incubated at 37 °C with 95% humidity and 5% CO_2 for 24 h before harvesting for subsequent analysis.

2.2. Cell Lysis, Protein Extraction, and Tryptic Digestion

Protein extraction from HCECs was achieved by lysing the cultures in urea buffer (7 M urea, 2 M thiourea, 40 mM Tris, pH 8.5) with 1% protease inhibitors (P8340, Millipore Sigma, Burlington, MA, USA). The lysates collected were then reduced by 5 mM dithiothreitol at 56 °C for 45 min, followed by alkylation with 15 mM iodoacetamide (IAA) for 30 min at room temperature in the dark. The proteins were then precipitated by mixing the lysate with 4 volumes of ice-cold acetone, followed by incubation for 8 h at −20 °C. The precipitated proteins were pelleted and collected by centrifugation for 30 min at 14,000*g*, 4 °C. The protein pellets were resuspended in urea buffer to a concentration of 1 μg/μL and then divided into two equal portions for Western blot and liquid chromatography tandem mass spectrometry (LC−MS/MS), respectively. One hundred micrograms of proteins from the cell lysates were digested with 4 μg of trypsin (#V5280; Promega, Madison, WI, USA) at 37 °C for 8 h. The peptides were then extracted and purified by passage through Pierce C_{18} Spin Columns (ThermoFisher) following the manufacturer's protocol. The peptides were dried using CentriVap Vacuum Concentrators (Labconco, Kansas City, MI, USA) with refrigeration and then redissolved in 30 μL of 0.1% formic acid before the proteomic analysis.

2.3. Proteomic Analysis by LC−Orbitrap-MS/MS (ThermoFisher) and Spectronaut

The tryptic peptides were analyzed by Orbitrap Fusion Lumos mass spectrometer coupled with an UltiMate 3000 RSLCnano and nanoelectrospray ionization system (ThermoFisher) in data-independent acquisition (DIA). Briefly, 1 μL of sample was loaded into an Aurora Ultimate nanoflow UHPLC column (120 Å, 1.7 μm, 25 × 75 μm; IonOpticks, Collingwood, VIC, Australia) equilibrated with 0.1% formic acid. The peptides were then fractionated by a linear elution gradient from 6% to 30% acetonitrile (ACN) for 120 min at a flow rate of 0.3 μL/min. The Orbitrap was operated in positive ion mode. The raw DIA data were imported to Spectronaut (V.18; Biognosys AG, Schlieren, Switzerland) for quantifying the relative abundances of the proteins in the samples. Proteomic analysis was conducted in library-free directDIA plus mode with the aid of the reviewed *Homo sapiens* protein sequence database (FASTA) from UniProt and gene ontology annotation (GOA) from the Gene Ontology (GO) database. FASTA contained 20,428 protein sequences including isoform, and GOA contained 19,653 entries (retrieved on 28-Dec-2023). The details for analyzing the

https://doi.org/10.1021/acs.jproteome.4c01046
J. Proteome Res. 2025, 24, 2771−2782

proteomic data with Spectronaut are provided in the Supporting Information and methods in the Supporting Information.

2.4. Free Amino Acid Profiling by LC−Triple Quadrupole-MS

HCECs were extracted with 150 μL of 0.1 M hydrochloric acid. After ultrasonication (30 s × 3 cycles, 24 kHz, 1s/1s pulse intervals, at 4 °C), the sample was centrifuged at 12,000*g* for 15 min at 4 °C, and the supernatant was harvested for amino acid profiling. The free amino acids in the supernatants were derivatized by the Kairos amino acid kit − low throughput 100+ (Waters, Milford, MA, USA) following the manufacturer's protocols. The samples were analyzed by multiple reaction monitoring (MRM) using Agilent 6460 Triple Quadrupole coupled with Agilent 1290 UHPLC (Agilent Technologies, Santa Clara, CA, USA). Two microliter samples were loaded into a CORTECS C_{18} column (90 Å, 1.6 μm, 2.1 m × 150 μm; Waters) equilibrated with 0.1% formic acid. The derivatized amino acids were fractionated by a 25 min elution gradient with 0.1% formic acid in ACN as previously described.[30] The MRM transitions of the derivatized amino acids monitored were based on the manufacturer's protocols. The raw data files were imported to MassHunter Workstation Software Quantitative Analysis (V.B.06.00; Agilent Technologies) for subsequent analysis. The concentrations of amino acids in the samples were calculated by peak areas of the parent and transition ions of the respective amino acids with reference to those of the internal standards (#186009051, Waters) and the calibrators (#186009193, Waters). The quantities of amino acids were then normalized by the number of HCECs in the corresponding samples.

2.5. Flow Cytometry

Flow cytometric analysis was performed to quantify the mitochondrial membrane potential ($\Delta\Psi m$), the level of mitochondrial superoxides, and glucose uptake. Briefly, 5 × 10^5 HCECs were seeded in a six-well culture plate and incubated overnight. The cultures were then treated with isotonic or hypertonic DMEM/F12 medium for 24 h and immediately analyzed using downstream flow cytometric measurement. The $\Delta\Psi m$ was measured by MitoTracker Red (#M46752, ThermoFisher). Briefly, HCECs were harvested and incubated with 50 nM MitoTracker Red either in isotonic or hypertonic DMEM/F12 (FBS-free) at 37 °C in the dark for 30 min. To measure mitochondrial superoxides, HCECs were harvested and incubated with 1 μM MitoSOX Red (#M36007, ThermoFisher) either in isotonic or hypertonic Hank's balanced salt solution (#14025092, ThermoFisher) at 37 °C in the dark for 30 min. After incubation with the fluorescent probes, HCECs were washed twice with the corresponding incubation medium without probes and resuspended before analysis using an Accuri C6 flow cytometer (BD Biosciences, Franklin Lakes, NJ, USA).

2.6. .Confocal Microscopy

The mitochondrial morphology of the HCECs was determined by visualization using confocal microscopy under either isotonic or hypertonic conditions. HCECs (1 × 10^5 cells per dish) were seeded in a confocal dish and incubated overnight. They were then treated with isotonic or hypertonic DMEM/F12 for 24 h, followed by mitochondrial labeling using 50 nM of MitoTracker Red CMXRos (#M46752, ThermoFisher) at 37 °C in the dark for 30 min. They were then washed twice with their corresponding incubation medium without the probe and imaged using an SP8 confocal microscope (Leica, Wetzlar, Germany). The mitochondrial morphology from the different treatments was processed by ImageJ software (NCBI, Bethesda, MD, USA) and quantified by ilastik software (V.1.3.0).[31]

2.7. Seahorse Mito-Stress Assay

The Seahorse mito-stress assay was performed to determine the metabolic profiles of HCECs upon different treatments. Oxidative phosphorylation of HCECs was measured using a Seahorse XFe 24 Extracellular Flux Analyzer default Mito-stress protocol (Agilent Technologies). In brief, 2.75 × 10^4 HCECs were seeded in a 24-well plate and incubated overnight. The next day, HCECs were treated with isotonic or hypertonic DMEM/F12 for 24 h, followed immediately by a downstream assay. HCECs were loaded to the analyzer and sequentially treated with 1.5 μM of oligomycin, 1.5 μM of carbonyl cyanide-*p*-trifluoromethoxyphenylhydrazone (FCCP), and finally with a 0.5 μM mixture of antimycin A and rotenone. Metabolic flux, in terms of oxygen consumption rate (OCR; pmol/min), was measured 3 times at 8 min intervals after the additions of each mitochondrial inhibitor. After the assay, the HCECs were immediately lysed with urea buffer to extract the total proteins. Protein concentrations were quantified with Bradford protein assay reagent (#5000006, Bio-Rad, Hercules, CA, USA). The OCR values of the samples were normalized with the total proteins.

2.8. RNA Extraction and Real-Time PCR

Extraction of the total RNA of the HECEs was performed with TRIzol reagent (#15596026, ThermoFisher) according to the manufacturer's instructions. The quantity and purity of the extracted RNA were determined by Varioskan LUX multimode microplate reader (ThermoFisher). This was followed by reverse transcription of RNA to complementary DNA (cDNA) using a high-capacity cDNA reverse transcription kit (#4368814, ThermoFisher) according to the manufacturer's instructions. The cDNA samples were then mixed with PowerTrack SYBR Green Master Mix (#A46012, ThermoFisher) and DNA primers (OriGene Technologies, Rockville, MD, USA). Real-time PCR was performed in StepOnePlus real-time PCR system (ThermoFisher) following the manufacturer's suggested conditions. The genes of interest and their corresponding primers are listed in the Supporting Information Table S1. The gene expression quantification was calculated by the $2^{-\Delta\Delta Ct}$ method. Glyceraldehyde 3-phosphate dehydrogenase was selected as the housekeeping gene for normalization.

2.9. SDS−PAGE and Western Blot

Three micrograms of proteins from each sample were loaded into a 10% SDS-polyacrylamide gel and separated according to their molecular weights using a Mini-PROTEAN Tetra electrophoresis system (Bio-Rad). After electrophoresis, the proteins in the SDS−polyacrylamide gel were transferred to an activated polyvinylidene difluoride (PVDF) membrane (0.2 μm pore size) using the Mini-PROTEAN Tetra electrophoresis system and Mini Trans-Blot module (Bio-Rad) at 4 °C. The membrane was then blocked with blocking buffer (5% w/v BSA, 0.1% Tween-20, 20 mM Tris, and 150 mM NaCl) at room temperature for 1 h with gentle shaking. After the blocking process, the membrane was probed with diluted primary antibody in blocking buffer for 8 h at 4 °C with gentle shaking. Mouse monoclonal anti-sodium-coupled neutral amino acid transporter (SNAT2) antibody (#sc-166366; Santa Cruz Biotechnology, Dallas, TX, USA), rabbit monoclonal anti-GLS antibody (#ab156876; Abcam, Cambridge, UK), and rabbit

https://doi.org/10.1021/acs.jproteome.4c01046
J. Proteome Res. 2025, 24, 2771−2782

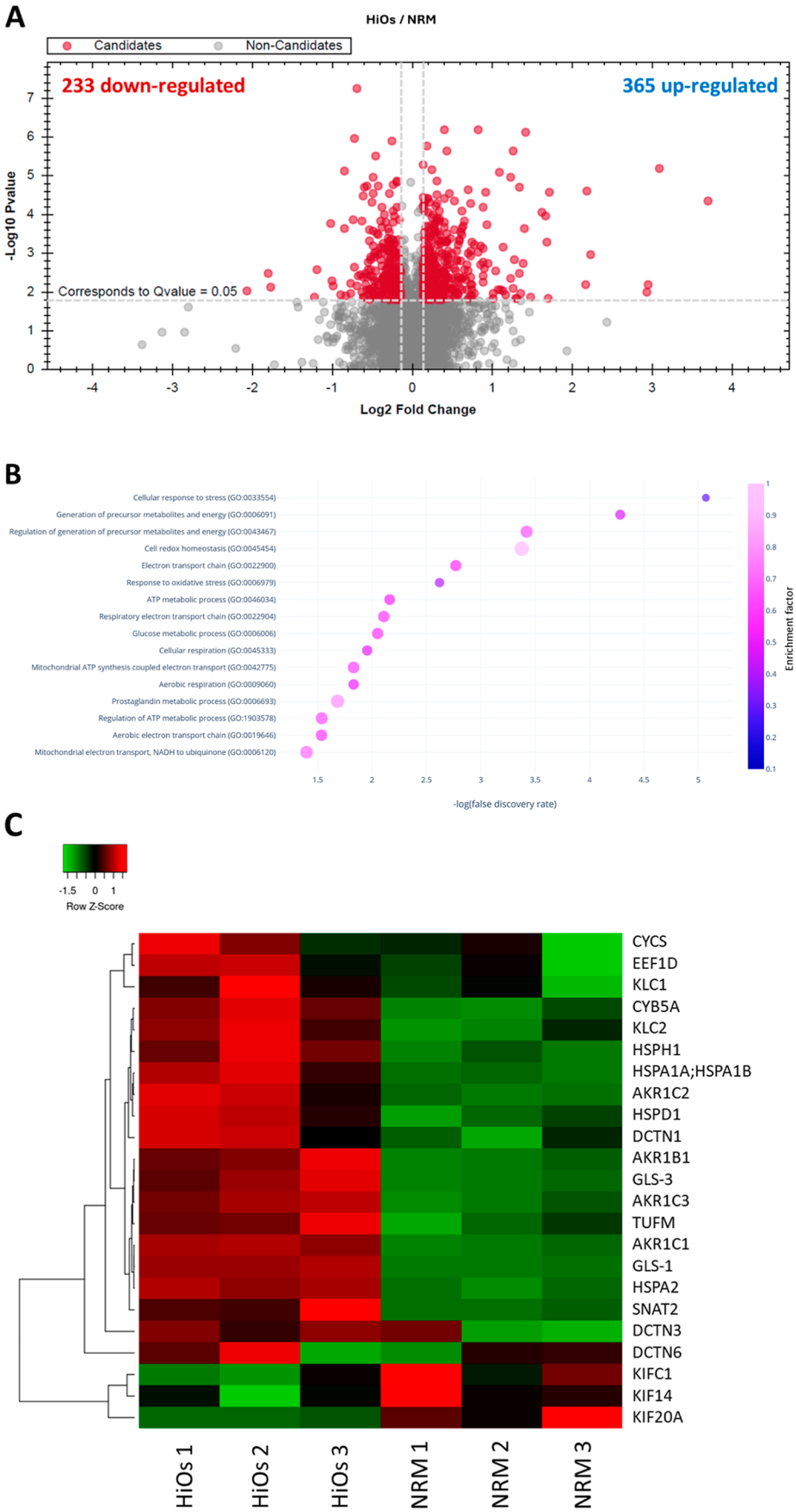

Figure 1. continued

https://doi.org/10.1021/acs.jproteome.4c01046
J. Proteome Res. 2025, 24, 2771−2782

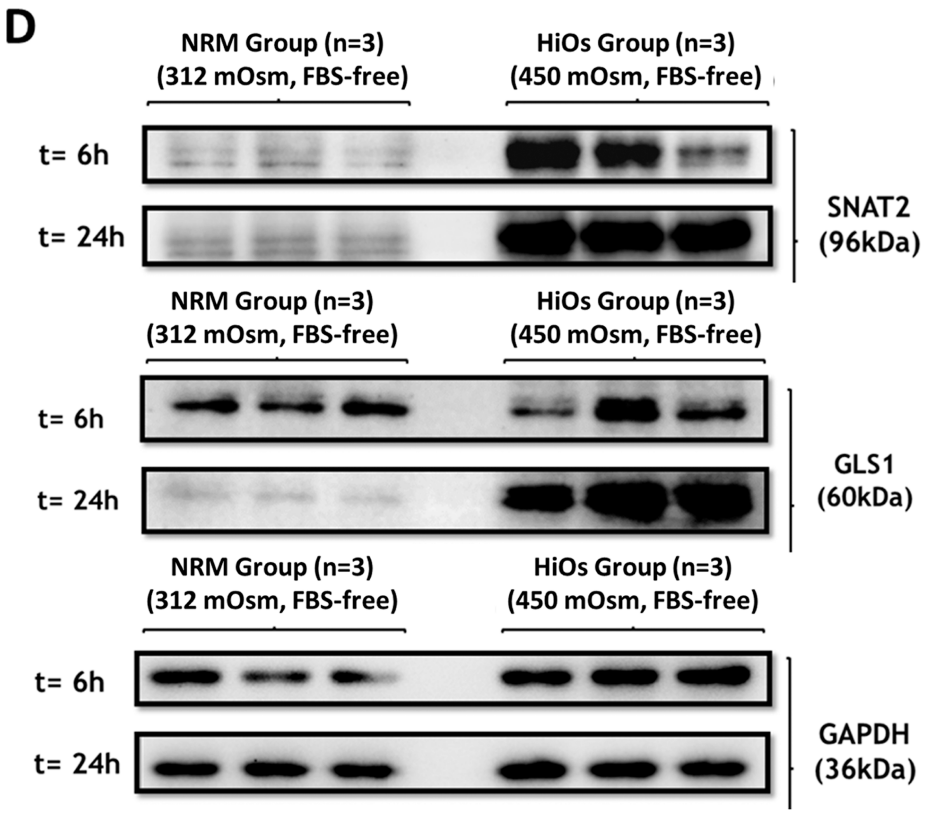

Figure 1. (A) Proteome changes of HCECs treated with isosmotic media (NRM) and hyperosmotic media (HiOs). (B) There were 233 and 365 proteins found to be increased and decreased (red circles), respectively, in HCECs upon hyperosmotic stress. The DEPs were mainly involved in mitochondrial functions, including the electron transport chain and redox hemostasis. (C) Enrichment factor was calculated as log10 (observed DEPs in a particular pathway/expected DEPs in that pathway). Most proteins related to hyperosmotic stress response were found to be increased (red) in HCECs under hyperosmotic stress, except KIFC1, KIF14, and KIF20A in the kinesin family. (D) The results from Western blots revealed that SNAT2 and GLS-1 began to increase in HCECs after 6 h exposure to hyperosmotic stress.

polyclonal anti-GAPDH antibody (#abs16, Sigma-Aldrich, St. Louis, MI, USA) were diluted with blocking buffer at the ratio of 1:1000, 1:1000, and 1:3000, respectively. The membrane was then washed 6 times for 5 min at room temperature with gentle shaking with TBS-T washing buffer (0.1% Tween-20, 20 mM Tris, and 150 mM NaCl). Goat HRP-linked antirabbit IgG antibody (#ab 205718, Abcam) and horse HRP-linked antimouse IgG antibody (#7076S, Cell Signaling Technology, Danvers, MA, USA) were diluted 1:3000 with blocking buffer. Depending on the primary antibody, the membrane was incubated with the corresponding diluted secondary antibody for 1 h at room temperature with gentle shaking. After washing 6 times, the membrane was incubated with SuperSignal West Pico PLUS chemiluminescent substrate (#34580, ThermoFisher) in the dark for 5 min at room temperature. The membrane was then transferred to ChemiDoc MP (Bio-Rad, USA) to capture the chemiluminescent signal.

2.10. Cell Viability Assay

HCECs were seeded into a 96-well plate with a density of 1×10^5 cells per well and incubated for 24 h. The cells were incubated with 200 μL of isotonic or hypertonic FBS-free medium for a further 24 h before the cell viability was assessed using a MTS assay kit (#ab197010, Abcam) to compare the viability of HCECs under different conditions. Briefly, 20 μL of MTS reagent was added to each well. After 2 h of incubation in standard culture conditions, the plate was briefly shaken, and the absorbance at 490 nm of each well was measured by the Varioskan LUX multimode microplate reader (ThermoFisher).

2.11. Total Glutathione Assay

HCECs were seeded into a 6-well plate with a density of 1×10^6 cells per well and incubated for 24 h. The cells were then incubated with 2 mL of isosmotic or hyperosmotic medium with or without glutamine for a further 24 h before the HCECs were collected for total glutathione assay. A glutathione assay kit (#ab239709, Abcam) was used to quantify the total intracellular glutathione of HCECs following the manufacturer's recommended protocol. After sample preparation, the absorbance at 405 nm of each well was measured. The quantity of total glutathione in the samples was calculated with reference to the standard curve established from glutathione standards and normalized with the amount of protein in the samples quantified by the Bradford protein assay.

2.12. Statistical Analysis

All experiments were performed on biological triplicates. Unpaired *t*-tests were also performed to test statistical significance between sample groups in all other biological assays. The results are presented as the mean ± SEM (standard error of the mean). The difference with a p value equal to or less than 0.05 (i.e., $p \leq 0.05$) was considered statistically significant. The statistical analyses were performed using Prism (V. 9.0; GraphPad Software, USA).

https://doi.org/10.1021/acs.jproteome.4c01046
J. Proteome Res. 2025, 24, 2771−2782

3. RESULTS

3.1. Changes in the Proteome and Free Amino Acid Profile of HCECs under Hyperosmotic Stress

After culturing HCECs in hyperosmotic medium, proteins were extracted for comparative proteomic analysis. There were 598 differentially expressed proteins (DEPs, $q < 0.05$, fold change > 1.1) identified between HCECs cultured in isosmotic media (NRM) and those cultured in the hyperosmotic media (HiOs, Figure 1A and Table S2). There were 365 DEPs, and 233 DEPs were found to be increased and decreased in the HiOs group compared to the NRM group, respectively. The functional analysis of the DEPs revealed that metabolism related to the electron transport chain (GO:0022900) and redox homeostasis (GO:0045454) in HCECs was impacted by the hyperosmotic stress (Figure 1B). This indicated that hyperosmotic stress might induce oxidative stress and alter the mitochondrial functions in HCECs, especially oxidative phosphorylation. Comparison with the NRM group revealed that a few protein families were significantly increased in the HiOs group. These included four proteins in the aldo-keto reductase family 1 (AKR1): AKR1B1 (P15121, also named aldose reductase), AKR1C1 (Q04828), AKR1C2 (P52895), and AKR1C3 (P42330) (Figure 1C). Isoforms of HSP 70 (P0DMV8, P0DMV9, and P54652), HSP 105 (Q92598), and mitochondrial HSP 60 (P10809) were also increased in the HiOs group. Furthermore, cytochrome *c* (CYCS; P99999) and cytochrome *b*5 (CYB5A; P00167), as well as elongation factor Tu (TUFM; P49411) and 1-delta (EEF1D; P29692-3), were increased in the HiOs group. Other protein families involved in mitochondrial dynamics and trafficking, as well as the dynein-dynactin complex, such as kinesin light chain 1 (KIF1; Q07866) and 2 (KIF2; Q9H0B6), and subunits of dynactin (O75935, O00399, and Q14203), were also increased when compared with the NRM group. Other than those, mitochondrial glutaminase (GLS-1; O94925), GLS-1 isoform 3 (GLS-3; O94925-3), and sodium-coupled neutral amino acid transporter 2 (SNAT2; Q96QD8) were significantly increased by at least 1.5-fold in the HiOs group (Figure 1C). SNAT2 and GLS-1 were found to be significantly increased in HCECs after cultured in the hyperosmotic media for 6 h (Figure 1D).

As the expressions of SNAT2 and GLS-1 were found to be increased, it implied that the free amino acid profile of the HiOs group might be altered. The free amino acid profiles of the NRM group and the HiOs group were quantified by multiple reaction monitoring. The results revealed that the free amino acid profiles of HCECs were altered by hyperosmotic stress. Intracellular amounts of the essential amino acids were significantly increased in the HiOs group (Table 1). Among these nonessential or conditionally essential amino acids, the intracellular amount of glutamine was almost doubled in the HiOs group compared to the NRM group. However, the intracellular levels of aspartic acid and L-ornithine were reduced in the HiOs group.

3.2. Mitochondrial Alterations in HCECs under Hyperosmotic Stress

As the functional proteomic analysis indicated that mitochondrial functions and redox homeostasis in HCECs might be altered by hyperosmotic stress, the effects of hyperosmotic stress on the mitochondrial membrane potential ($\Delta\Psi m$), superoxide level, and mitochondrial morphology of the HCECs were investigated. The mitochondrial superoxide level and $\Delta\Psi m$ of the HiOs group were found to be increased significantly (Figure 2A,B). The mitochondrial morphology in the HiOs group showed alterations in terms of number, size, branches, and length when compared to the NRM group (Figure 2C). The HiOs group had a higher number but smaller mitochondria (Figure 2D,E). The mitochondria of the HiOs group were highly branched, but their average length and maximum length were shorter than those in the NRM group (Figure 2F,H). These fragmented morphological characteristics indicated that HCECs underwent mitochondrial fission under the hyperosmotic stress. Thus, a mito-stress assay was conducted to investigate the effects of hyperosmotic stress on oxidative phosphorylation in HCECs (Figure 3A). As expected, the basal respiration of the HiOs group was reduced significantly compared to that of the NRM group (Figure 3A,B). In addition, the increased coupling efficiency and reduced proton leak in the HiOs group implied that the oxygen in basal respiration was largely consumed for producing adenosine triphosphates (ATPs) by mitochondrial oxidative phosphorylation in the HiOs group (Figure 3C,E). Interestingly, the maximal respiration in the HiOs group remained similar to the NRM group (Figure 3F). In contrast, the spare respiratory capacity of the HiOs group was significantly higher than the NRM group (Figure 3G). These results indicated that the mitochondria in HCECs after the hyperosmotic stresses were still capable of increasing the rate of respiration to respond to a higher energy demand.

Table 1. Amino Acid Profiles of the NRM Group and the HiOs Group

amino acids and their derivatives	normalized intracellular concentration (mean ± SEM, pM)[a] NRM group	HiOs group	significance[b]
leucine	10.80 ± 1.09	23.74 ± 1.34	[c]
tryptophan	2.14 ± 0.23	4.13 ± 0.16	[c]
isoleucine	9.34 ± 1.19	21.38 ± 1.40	[c]
valine	10.64 ± 1.15	23.64 ± 1.65	[c]
histidine	2.86 ± 0.48	6.51 ± 0.35	[c]
phenylalanine	5.92 ± 0.80	13.60 ± 0.98	[c]
tyrosine	5.69 ± 0.74	12.08 ± 0.76	[c]
threonine	14.12 ± 1.47	35.83 ± 3.36	[c]
hydroxyproline	15.63 ± 2.87	40.90 ± 5.56	[d]
methionine	1.81 ± 0.27	2.84 ± 0.08	[d]
L-ornithine	0.93 ± 0.12	2.01 ± 0.28	[d]
aspartic acid	28.40 ± 0.89	24.74 ± 0.76	[d]
glutamine	40.30 ± 8.38	78.34 ± 8.93	[d]
lysine	8.00 ± 0.79	11.04 ± 0.80	ns
proline	7.73 ± 1.05	11.29 ± 0.81	ns
glutamic acid	90.74 ± 11.85	126.95 ± 7.31	ns
arginine	4.85 ± 0.70	6.95 ± 0.53	ns
asparagine	2.90 ± 0.30	3.70 ± 0.25	ns
taurine	0.79 ± 0.13	1.04 ± 0.13	ns
glycine	75.05 ± 53.86	42.80 ± 27.31	ns
alanine	6.93 ± 0.29	7.10 ± 0.35	ns
β-alanine	26.85 ± 3.12	27.71 ± 1.62	ns
serine	12.22 ± 0.24	12.34 ± 0.56	ns

[a]SEM: standard error of measurement, 3 biological replicates were conducted. [b]ns: not significant. [c]$p < 0.05$. [d]$p < 0.005$.

3.3. Increased Expression of SNAT2 and GLS-1 in HCECs Was Induced by Hyperosmotic Stress but Not by Glutamine Deprivation

To validate glutamine reliance of HCECs, HCECs cultured with either isosmotic medium or hyperosmotic medium were further subjected to glutamine deprivation. The basal respiration and

https://doi.org/10.1021/acs.jproteome.4c01046
J. Proteome Res. 2025, 24, 2771−2782

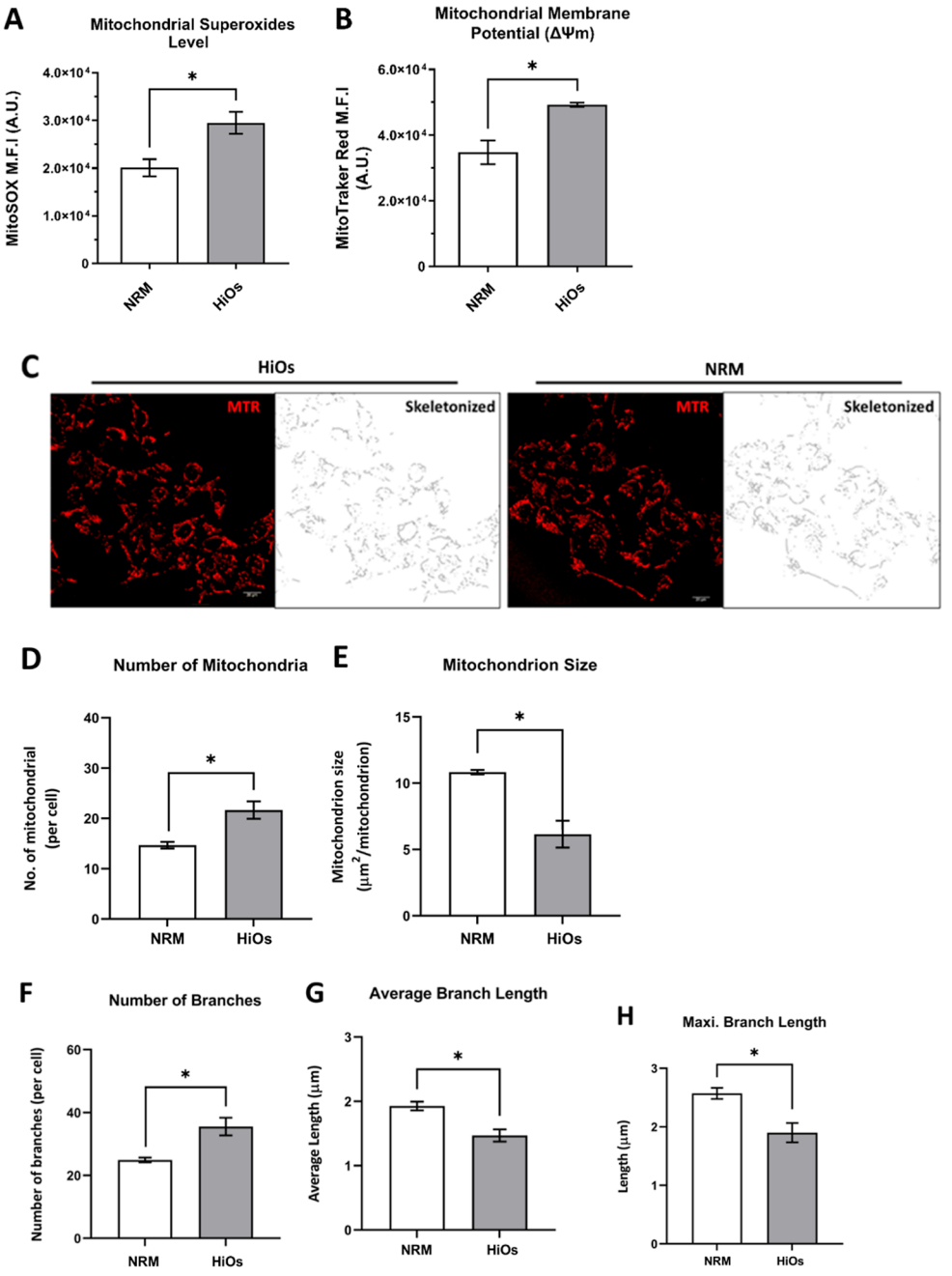

Figure 2. Mitochondrial alterations in HCECs cultured under normal osmotic conditions (NRM) and under hyperosmotic stress (HiOs). The mitochondrial superoxide level (A) and $\Delta\Psi m$ (B) of the HiOs group (gray) increased significantly. The morphologies of the mitochondria in the HiOs group were captured by confocal microscopy (C). When compared to the NRM group, the mitochondrial morphology in the His group showed significant alterations in terms of the number of mitochondria (D), mitochondrial size (E), number of branches (F), and length of branch (G,H). Results are presented as the mean ± SEM and *: $p \leq 0.05$ ($n = 3$).

ATP production of HECEs cultured in the isosmotic medium without glutamine (NRM -Gln) were found to be reduced, which indicated that glutamine could be used as the substrate for oxidative phosphorylation in HCECs (Figure 3B,C). Additionally, both the NRM -Gln group and HECEs cultured in the hyperosmotic medium without glutamine (HiOs -Gln) failed to increase the rate of respiration upon treatment with carbonyl cyanide-*p*-trifluoromethoxyphenylhydrazone (FCCP) (Figure 3G). Aligned with the results from the mito-stress assay, the viability and intracellular glutathione concentration of the HiOs -Gln group were found to be significantly reduced compared to the NRM group (Figure 4A,B). Moreover, the decreases in the viability and intracellular glutathione concentration of HCECs were further aggravated under glutamine-deprived hyperosmotic conditions. The concentration of glutamine supplied was found to be directly correlated to the survival of HCECs in both normal and hyperosmotic conditions (Figure S1). As glutamine deprivation affected oxidative phosphorylation, glutathione production, and reduced viability of HCECs under hyperosmotic stress, it was suspected that glutamine deprivation might also affect the expressions of SNAT2 and GLS-1 in HCECs, similar to hyperosmotic stress. Surprisingly, expressions of SNAT2 and GLS-1 only increased in the HiOs group and the HiOs -Gln group but not in the NRM group and the

https://doi.org/10.1021/acs.jproteome.4c01046
J. Proteome Res. 2025, 24, 2771−2782

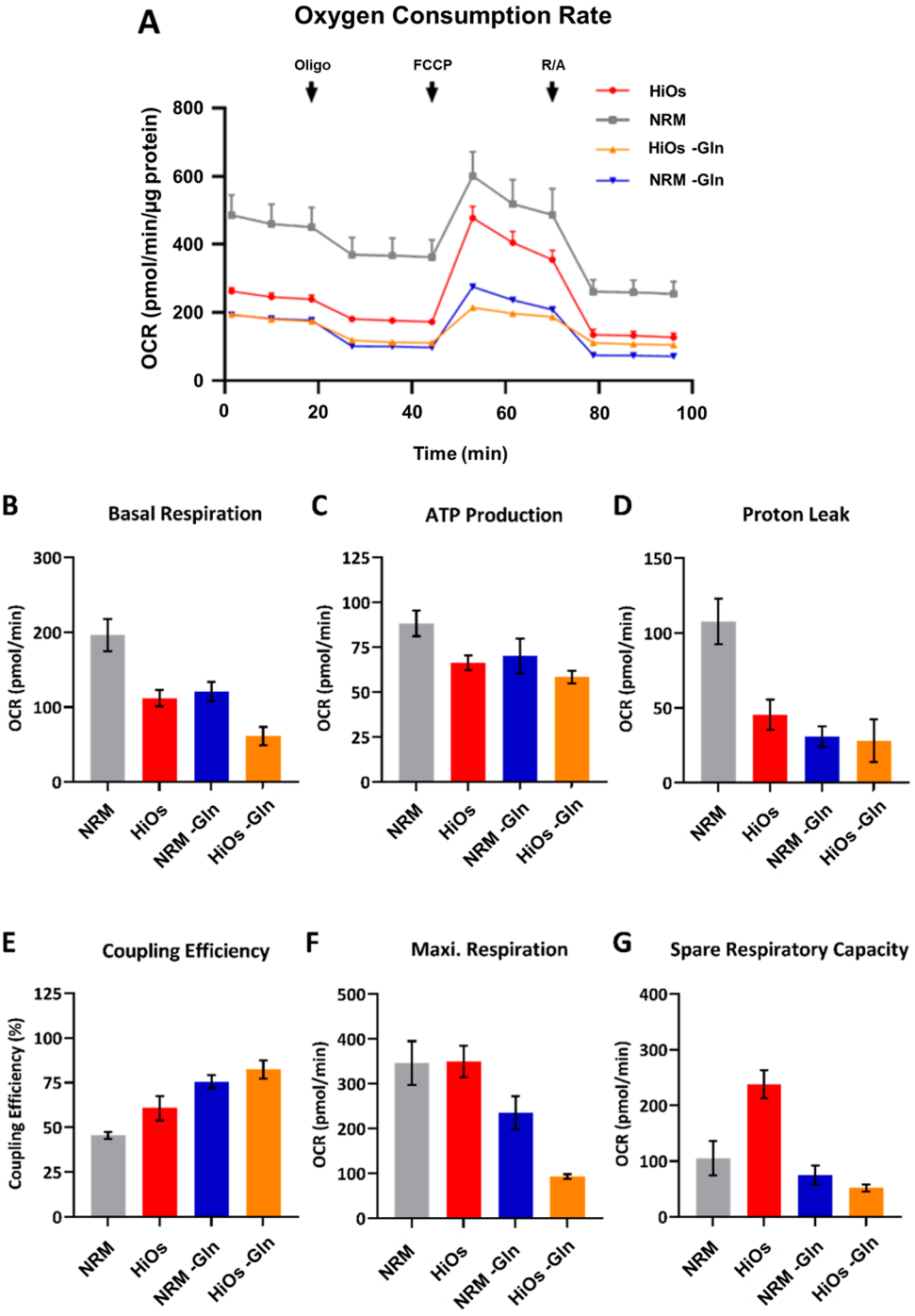

Figure 3. Respiration alterations in HCECs cultured in the isosmotic medium (NRM), the hyperosmotic medium (HiOs), the isosmotic medium without glutamine (NRM -Gln), and the hyperosmotic medium without glutamine (HiOs -Gln). The oxygen consumption rates were found to vary among 4 conditions after treatments with oligomycin (Oligo), carbonyl cyanide-*p*-trifluoromethoxyphenylhydrazone (FCCP), as well as rotenone and antimycin A (R/A) in the mito-stress assay (A). The basal respiration (B), ATP production (C), and proton leak (D) of NRM-HCEC were higher than the other groups. The coupling efficiencies of the HiOs group and the HiOs -Gln group were increased (E). The maximal respiration in the HiOs group remained similar to the NRM group, while the maximal respiration was reduced in the NRM -Gln group and the HiOs -Gln group (F). The spare respiratory capacity of the HiOs group was significantly higher than the other groups (G).

NRM -Gln group at both transcriptional (Figure 4C,D) and translational levels (Figure 4E,F). In addition, the expression levels of TNF-α and IL-1β exhibited increased expression in the HiOs group and the HiOs -Gln group (Figure S2A,B). The heightened presence of these inflammatory markers serves as a clear indication of the successful induction of dry eye condition in HCECs.

4. DISCUSSION

This proteomic study revealed that HCECs increased the expression of HSP 70, AKR1B1, and elongation factors upon the hyperosmotic stress (Figure 1C). These expressional changes observed in HCECs were similar to those of murine inner medullary collecting tube 3 cells, the epithelial cells of the thick ascending limb of Henle's loop, and murine embryonic

https://doi.org/10.1021/acs.jproteome.4c01046
J. Proteome Res. 2025, 24, 2771−2782

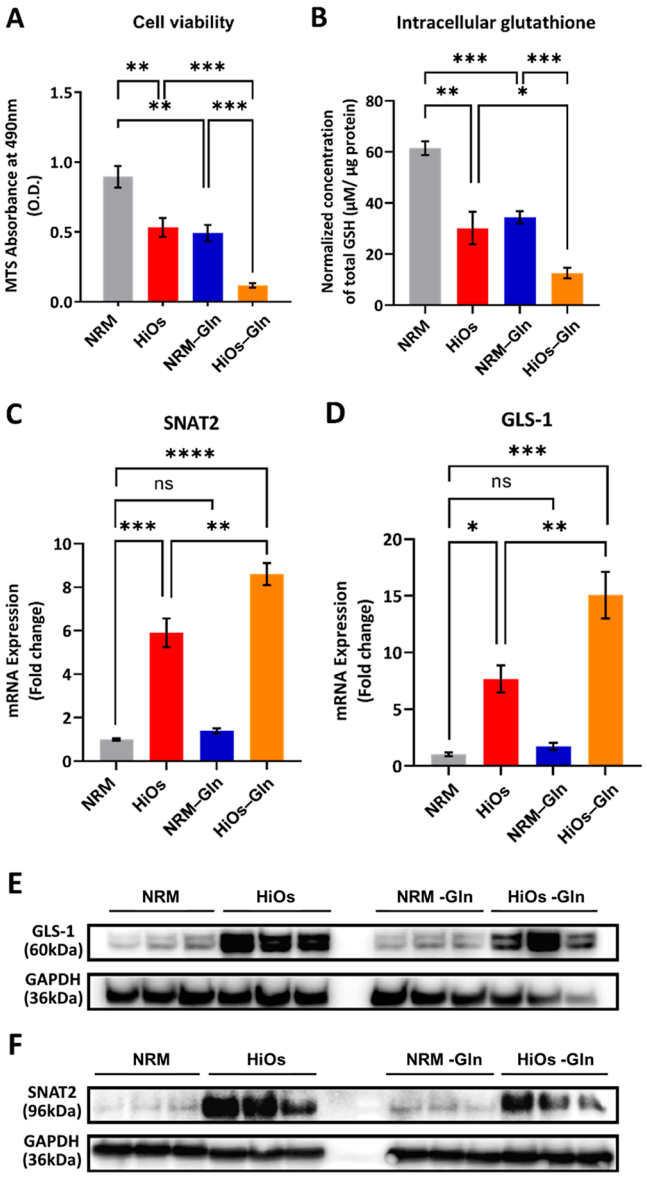

Figure 4. Cell viability, intracellular glutathione level, and expression of SNAT2 and GLS-1 in HCECs under normal osmotic conditions (NRM), hyperosmotic stress (HiOs), normal osmotic conditions without glutamine (NRM -Gln), and hyperosmotic stress without glutamine (HiOs -Gln). The viability (A) and intracellular glutathione levels (B) of the HiOs group and the HiOs -Gln group were found to be significantly reduced compared to the NRM group. Expression of SNAT2 and GLS-1 were significantly increased in the HiOs group (red) and the HiOs -Gln group (orange) but not in the NRM group (gray) and the NRM -Gln group (blue) at both transcriptional (C,D) and translational levels (E,F). (ns: not significant; *: $p < 0.05$; **: $p < 0.005$; ***: $p < 0.0005$).

fibroblasts under the hyperosmotic stress.[16,18,21] A recent study of human conjunctival epithelial cells reported that the expressions of multiple elongation factors, aldose reductase, and HSP 70 were dysregulated after hyperosmotic stress.[32] These concluded that the increased expression of HSP 70, aldose reductase, and elongation factors may be common stress responses in different mammalian cell types under hyperosmotic stress. In addition to those proteins, the current study's findings also demonstrated that expressions of SNAT2 and GLS-1 were increased in HCECs after exposure to hyperosmotic stress for 6 h (Figure 1D) but not after the glutamine deprivation (Figure 4C,F).

SNAT2 is one of the system A transporters encoded by the solute carrier (SLC) 38 gene family.[33] SNAT2 transports a sodium ion (Na^+) along with a zwitterionic neutral amino acid, like glutamine, glycine, alanine, proline, and serine. SNAT2 was found to be expressed in multiple organs and tissues.[34] The expression of SNAT2 was known to be induced in response to deprivations of both essential and nonessential amino acids.[35−37] A recent study revealed that the presence of extracellular Na^+ was crucial for inducing the expression of SNAT2 in HeLa cells under the amino acid deprivation.[38] In the absence of extracellular Na^+, HeLa failed to increase expression of SNAT2 under the amino acid deprivation. This recent finding could partially account for the increased expression of SNAT2 in the HiOs group and the HiOs -Gln group but not in the NRM group and the NRM -Gln group. As the expression of SNAT2 might be partially regulated by extracellular Na^+, SNAT2 was only highly expressed in HCECs under hyperosmotic stress (increased NaCl concentration in culture medium) but not upon glutamine deprivation.

Among the neutral amino acids known to be transported by SNAT2, only the intracellular concentration of glutamine was found to be significantly increased in the HiOs group (Table 1). In addition, other essential amino acids were found to be accumulated in HCECs upon the hyperosmotic stress (Table 1). The changes of the free amino acid profiles of HCECs and human conjunctival epithelial cells were found to be similar after exposure to the hyperosmotic stress.[32] This implied that both human corneal and conjunctival epithelia might respond similarly to the hyperosmotic stress. The neutral amino acid uptake via SNAT2 is not only used for biosynthetic and bioenergetic processes but also acts as osmolytes to control the intracellular osmolarity and cell volume.[39] The accumulation of specific amino acids, notably glutamine, proline, and glutamate, has been shown to facilitate cell volume recovery in human saphenous vein endothelial cells and fibroblasts following hyperosmotic stress, thereby alleviating cell shrinkage.[40,41] Conversely, glutamine deprivation has been demonstrated to induce cell shrinkage and subsequent apoptosis in human promyeloblasts and leukemic lymphoblasts.[42] Taken together, these findings suggested that glutamine serves as a key osmolyte involved in osmoregulation and cell volume control across different types of human cells. The current study demonstrates that HCECs exhibit a specific osmoregulatory mechanism characterized by the accumulation of intracellular glutamine via the increased expression of SNAT2. Therefore, the increased expression of SNAT2 is likely a specific osmoregulatory response of HCECs under the hyperosmotic stress. As such, SNAT2 may serve as a potential biomarker for monitoring early pathogenesis or progression of DES in human corneal epithelium.

The fragmentation of mitochondria and the production of the mitochondrial superoxide in the HCECs induced by the hyperosmotic stress were found to be similar to the findings from other studies on corneal epithelial cells (Figure 2).[43] Mitochondrial fission fragments damaged a mitochondrion into a functional mitochondrion and a dysfunctional mitochondrion; subsequently, the dysfunctional mitochondrion could be selectively degraded by mitophagy.[44−46] The functional mitochondria from the fission in the HiOs group were still capable of increasing $\Delta\Psi m$ and coupling efficiency, as well as reducing the proton leak to maintain ATP production (Figures

https://doi.org/10.1021/acs.jproteome.4c01046
J. Proteome Res. 2025, 24, 2771−2782

2B and 3C−E). As SNAT2 transports glutamine to cells and GLS-1 facilitates the conversion of glutamine to glutamate, these glutamates could ultimately be used for the production of α-ketoglutarate as an alternate metabolic fuel to the mitochondrial oxidative phosphorylation[47] or for the production of glutathione.[45] With high intracellular glutamine imported by SNAT2, the HiOs group could still increase the respiratory rate (spare respiratory capacity) to meet the energy demand by converting glutamine to glutamate via the upregulated GLS-1 for the tricarboxylic acid cycle and oxidative phosphorylation (Figure 3G).[47,48] Under the glutamine deprivation, the HiOs -Gln group had a low maximum respiratory rate and spare respiratory capacity as expected (Figure 3F,G). Although the intracellular glutamine concentration increased in the HiOs group, the intracellular glutathione concentration was significantly reduced (Figure 4B). This indicates that the intracellular glutamine may not be directed into glutathione production but act as an energy source and osmolyte to regulate the osmolarity of HCECs under the hyperosmotic pressure. As a result, the accumulation of mitochondrial superoxide and mitochondrial fission may lead to the subsequent release of cytochrome *c* from mitochondria into the cytosol, causing apoptosis.[49,50] Thus, the viability of the HiOs group was found to be significantly reduced compared to the NRM group (Figure 4A). Moreover, the viability of the HiOs -Gln group was significantly lower than the others due to the combined effects of the glutamine deprivation, decreased glutathione production, and the hyperosmotic stress. As HCECs relied on glutamine for energy metabolism and increased the expression of GLS-1 to convert glutamine to glutamate for respiration under the hyperosmotic stress, GLS-1 should be considered as a potential biomarker for monitoring the pathogenesis or progression of DES in the human corneal epithelium.

Tears have been found to be rich in free amino acids, especially glutamine and taurine.[51] It is believed that corneal epithelium uptakes glutamine from tear fluid to partially meet its bioenergetic and biosynthetic demands. Among the DES patients, some may fail to produce a sufficient amount of tears due to dysfunction of the lacrimal glands. The others may experience an increase in the evaporation rate of the tear film due to dysfunction of meibomian glands; as a consequence, the concentrations of free amino acids, ions, and other metabolites in tears collected from some of the DES patients were reported to be higher than those from healthy subjects, resulting in hyperosmotic tear fluid.[52,53] To adapt hyperosmotic tears, the current findings suggest that the corneal epithelium could increase SNAT2 expression to enhance uptake of glutamine for osmoregulation and increase GSL-1 expression to increase conversion of glutamine to glutamate to meet bioenergetic demands. However, it is doubted that the supply of glutamine to the corneal epithelium from the unstable tear film might be insufficient, and the glutamine deprivation might induce mitochondrial fission, causing apoptosis in the corneal epithelium.[54,55] Thus, supplementations of amino acids and other derivatives of amino acids have been considered as a potential treatment for DES, attempting to maintain homeostasis of the ocular surface.[46,56,57] Taken together, future developments of eyedrop formulations should address both the hyperosmolarity of the unstable tear film and the free amino acid requirements of the corneal epithelium to restore or maintain the health of the corneal epithelium of DES sufferers.

■ ASSOCIATED CONTENT

Data Availability Statement

Proteomic data of this study was deposited to Japan ProteOme STandard Repository (jPOST). The accession numbers of this proteome data are PXD054330 for ProteomeXchange and JPST003233 for jPOST.

Supporting Information

The Supporting Information is available free of charge at https://pubs.acs.org/doi/10.1021/acs.jproteome.4c01046.

Methods related to proteomic data analysis with Spectronaut, summary of the primers used in real-time PCR, cell viability of the NRM group and the HiOs 28 group, expression levels of TNF-α and IL-1β, images of entire Western blot membranes, and table legends of supplementary Table S2 (PDF)

Details of the differentially expressed proteins identified in the proteomic analysis (XLSX)

■ AUTHOR INFORMATION

Corresponding Author

Hang-Kin Kong − *Centre for Eye and Vision Research, Hong Kong SAR 999077, China; Department of Food Science and Nutrition, Faculty of Science, The Hong Kong Polytechnic University, Hong Kong SAR 999077, China;* orcid.org/0000-0002-1047-7051; Email: hang-kin.kong@polyu.edu.hk

Authors

Kenrick Kai-yuen Chan − *Centre for Eye and Vision Research, Hong Kong SAR 999077, China;* orcid.org/0000-0002-0841-5177

Alan Chun-kit Lee − *Department of Applied Biology and Chemical Technology, Faculty of Science, The Hong Kong Polytechnic University, Hong Kong SAR 999077, China;* orcid.org/0000-0001-9611-910X

Shing-yan Roy Chung − *Centre for Eye and Vision Research, Hong Kong SAR 999077, China; School of Optometry, Faculty of Health and Social Sciences, The Hong Kong Polytechnic University, Hong Kong SAR 999077, China*

Man-sau Wong − *Centre for Eye and Vision Research, Hong Kong SAR 999077, China; Department of Food Science and Nutrition, Faculty of Science, The Hong Kong Polytechnic University, Hong Kong SAR 999077, China*

Chi-wai Do − *Centre for Eye and Vision Research, Hong Kong SAR 999077, China; School of Optometry, Faculty of Health and Social Sciences, The Hong Kong Polytechnic University, Hong Kong SAR 999077, China*

Thomas Chuen Lam − *Centre for Eye and Vision Research, Hong Kong SAR 999077, China; School of Optometry, Faculty of Health and Social Sciences, The Hong Kong Polytechnic University, Hong Kong SAR 999077, China;* orcid.org/0000-0002-3511-5620

Complete contact information is available at: https://pubs.acs.org/10.1021/acs.jproteome.4c01046

Author Contributions

⊥K.K.-y.C. and A.C.-k.L. contributed equally to this work. **Kenrick Kai-Yuen Chan**: methodology, investigation, formal analysis, and writing—original draft. **Alan Chun-kit Lee**: methodology, investigation, formal Analysis, and writing—

https://doi.org/10.1021/acs.jproteome.4c01046
J. Proteome Res. 2025, 24, 2771−2782

original draft. **Roy Chung**: investigation, formal analysis, and writing—original draft. **Man-sau Wong**: funding acquisition and supervision. **Chi-wai Do**: funding acquisition and supervision. **Thomas Chuen Lam**: funding acquisition and supervision. **Hang-Kin Kong**: conceptualization, methodology, supervision, project administration, and writing—review and editing.

Funding

This work was financially supported by the InnoHK initiative of the Innovation and Technology Commission of the Hong Kong Special Administrative Region Government and Research Centre for SHARP Vision at the Hong Kong Polytechnic University.

Notes

The authors declare no competing financial interest.

■ ACKNOWLEDGMENTS

The authors gratefully acknowledge technical support from the University Research Facility in Chemical and Environmental Analysis (UCEA) and the University Research Facility in Life Sciences (ULS) of the Hong Kong Polytechnic University. The authors would also like to thank Dr. Maureen Valerie Boost (technical writer, PolyU, Hong Kong) for her diligent proofreading of the article.

■ REFERENCES

(1) Papas, E. B. The global prevalence of dry eye disease: A Bayesian view. *Ophthalmic Physiol. Opt.* **2021**, *41* (6), 1254−1266.
(2) Craig, J. P.; Nichols, K. K.; Akpek, E. K.; Caffery, B.; Dua, H. S.; Joo, C. K.; Liu, Z.; Nelson, J. D.; Nichols, J. J.; Tsubota, K.; Stapleton, F. TFOS DEWS II Definition and Classification Report. *Ocul. Surf.* **2017**, *15* (3), 276−283.
(3) Chhadva, P.; Goldhardt, R.; Galor, A. Meibomian Gland Disease: The Role of Gland Dysfunction in Dry Eye Disease. *Ophthalmology* **2017**, *124* (11), S20−S26.
(4) Lim, E. W. L.; Chong, C. C. Y.; Nusinovici, S.; Fenwick, E.; Lamoureux, E. L.; Sabanayagam, C.; Cheng, C. Y.; Tong, L. Relationship between dry eye symptoms and quality of life: associations and mediation analysis. *Br. J. Ophthalmol.* **2023**, *107* (11), 1606−1612.
(5) Tovar, A. A.; Frankel, S. T.; Galor, A.; Sabater, A. L. Living with Dry Eye Disease and its Effects on Quality of Life: Patient, Optometrist, and Ophthalmologist Perspectives. *Ophthalmol. Ther.* **2023**, *12* (5), 2219−2226.
(6) Yamaguchi, T. Inflammatory Response in Dry Eye. *Investig. Ophthalmol. Vis. Sci.* **2018**, *59* (14), DES192−DES199.
(7) Liu, H.; Begley, C.; Chen, M.; Bradley, A.; Bonanno, J.; McNamara, N. A.; Nelson, J. D.; Simpson, T. A link between tear instability and hyperosmolarity in dry eye. *Investig. Ophthalmol. Vis. Sci.* **2009**, *50* (8), 3671−3679.
(8) Baudouin, C.; Aragona, P.; Messmer, E. M.; Tomlinson, A.; Calonge, M.; Boboridis, K. G.; Akova, Y. A.; Geerling, G.; Labetoulle, M.; Rolando, M. Role of Hyperosmolarity in the Pathogenesis and Management of Dry Eye Disease: Proceedings of the OCEAN Group Meeting. *Ocul. Surf.* **2013**, *11* (4), 246−258.
(9) Yeh, S.; Song, X. J.; Farley, W.; Li, D. Q.; Stern, M. E.; Pflugfelder, S. C. Apoptosis of ocular surface cells in experimentally induced dry eye. *Investig. Ophthalmol. Vis. Sci.* **2003**, *44* (1), 124−129.
(10) Yang, L.; Zhang, S.; Duan, H.; Dong, M.; Hu, X.; Zhang, Z.; Wang, Y.; Zhang, X.; Shi, W.; Zhou, Q. Different Effects of Pro-Inflammatory Factors and Hyperosmotic Stress on Corneal Epithelial Stem/Progenitor Cells and Wound Healing in Mice. *Stem Cells Transl. Med.* **2019**, *8* (1), 46−57.
(11) Li, J.; Yang, K.; Pan, X.; Peng, H.; Hou, C.; Xiao, J.; Wang, Q. Long Noncoding RNA MIAT Regulates Hyperosmotic Stress-Induced Corneal Epithelial Cell Injury via Inhibiting the Caspase-1-Dependent Pyroptosis and Apoptosis in Dry Eye Disease. *J. Inflamm. Res.* **2022**, *15*, 3269−3283.
(12) Lian, L.; Ye, X.; Wang, Z.; Li, J.; Wang, J.; Chen, L.; Reinach, P. S.; Ma, X.; Chen, W.; Zheng, Q. Hyperosmotic stress-induced NLRP3 inflammasome activation via the mechanosensitive PIEZO1 channel in dry eye corneal epithelium. *Ocul. Surf.* **2025**, *36*, 106−118.
(13) Hung, N.; Kang, E. Y.; Lee, T. W.; Chen, T. H.; Shyu, Y. C.; Sun, C. C. The Risks of Corneal Surface Damage in Aqueous-Deficient Dry Eye Disease: A 17-Year Population-Based Study in Taiwan. *Am. J. Ophthalmol.* **2021**, *227*, 231−239.
(14) Abou Shousha, M.; Wang, J.; Kontadakis, G.; Feuer, W.; Canto, A. P.; Hoffmann, R.; Perez, V. L. Corneal epithelial thickness profile in dry-eye disease. *Eye* **2020**, *34* (5), 915−922.
(15) Michea, L.; Ferguson, D. R.; Peters, E. M.; Andrews, P. M.; Kirby, M. R.; Burg, M. B. Cell cycle delay and apoptosis are induced by high salt and urea in renal medullary cells. *Am. J. Physiol.: Renal Physiol.* **2000**, *278* (2), F209−F218.
(16) Valkova, N.; Kultz, D. Constitutive and inducible stress proteins dominate the proteome of the murine inner medullary collecting duct-3 (mIMCD3) cell line. *Biochim. Biophys. Acta* **2006**, *1764* (6), 1007−1020.
(17) Santos, B. C.; Pullman, J. M.; Chevaile, A.; Welch, W. J.; Gullans, S. R. Chronic hyperosmolarity mediates constitutive expression of molecular chaperones and resistance to injury. *Am. J. Physiol.: Renal Physiol.* **2003**, *284* (3), F564−F574.
(18) Dihazi, H.; Asif, A. R.; Agarwal, N. K.; Doncheva, Y.; Muller, G. A. Proteomic analysis of cellular response to osmotic stress in thick ascending limb of Henle's loop (TALH) cells. *Mol. Cell. Proteomics* **2005**, *4* (10), 1445−1458.
(19) Singh, M. K.; Shin, Y.; Ju, S.; Han, S.; Choe, W.; Yoon, K. S.; Kim, S. S.; Kang, I. Heat Shock Response and Heat Shock Proteins: Current Understanding and Future Opportunities in Human Diseases. *Int. J. Mol. Sci.* **2024**, *25* (8), 4209.
(20) Ferrarett, A.; Negri, A.; Giuliani, A.; De Grada, L.; Conti, A. M. F.; Ronchi, S. Aldose reductase is involved in long-term adaptation of EUE cells to hyperosmotic stress. *Biochim. Biophys. Acta Mol. Cell Res.* **1993**, *1175* (3), 283−288.
(21) Shim, E. H.; Kim, J. I.; Bang, E. S.; Heo, J. S.; Lee, J. S.; Kim, E. Y.; Lee, J. E.; Park, W. Y.; Kim, S. H.; Kim, H. S.; Smithies, O.; Jang, J. J.; Jin, D. I.; Seo, J. S. Targeted disruption of hsp70.1 sensitizes to osmotic stress. *EMBO Rep.* **2002**, *3* (9), 857−861.
(22) Xu, W.; Hong, S. J.; Zhong, A.; Xie, P.; Jia, S.; Xie, Z.; Zeitchek, M.; Niknam-Bienia, S.; Zhao, J.; Porterfield, D. M.; Surmeier, D. J.; Leung, K. P.; Galiano, R. D.; Mustoe, T. A. Sodium channel Nax is a regulator in epithelial sodium homeostasis. *Sci. Transl. Med.* **2015**, *7* (312), 312ra177.
(23) Seltmann, K.; Meyer, M.; Sulcova, J.; Kockmann, T.; Wehkamp, U.; Weidinger, S.; Auf dem Keller, U.; Werner, S. Humidity-regulated CLCA2 protects the epidermis from hyperosmotic stress. *Sci. Transl. Med.* **2018**, *10* (440), No. eaao4650.
(24) Sanger, C. S.; Cernakova, M.; Wietecha, M. S.; Garau Paganella, L.; Labouesse, C.; Dudaryeva, O. Y.; Roubaty, C.; Stumpe, M.; Mazza, E.; Tibbitt, M. W.; Dengjel, J.; Werner, S. Serine protease 35 regulates the fibroblast matrisome in response to hyperosmotic stress. *Sci. Adv.* **2023**, *9* (35), No. eadh9219.
(25) Wang, L.; Dai, W.; Lu, L. Hyperosmotic stress-induced corneal epithelial cell death through activation of Polo-like kinase 3 and c-Jun. *Investig. Ophthalmol. Vis. Sci.* **2011**, *52* (6), 3200−3206.
(26) Luo, L.; Li, D. Q.; Pflugfelder, S. C. Hyperosmolarity-induced apoptosis in human corneal epithelial cells is mediated by cytochrome c and MAPK pathways. *Cornea* **2007**, *26* (4), 452−460.
(27) Zheng, Q.; Tan, Q.; Ren, Y.; Reinach, P. S.; Li, L.; Ge, C.; Qu, J.; Chen, W. Hyperosmotic Stress−Induced TRPM2 Channel Activation Stimulates NLRP3 Inflammasome Activity in Primary Human Corneal Epithelial Cells. *Biochim. Biophys. Acta Mol. Cell Res.* **2018**, *59* (8), 3259−3268.
(28) Wong, K.-Y.; Liu, Y.; Wong, M.-S.; Liu, J. Cornea-SELEX for aptamers targeting the surface of eyes and liposomal drug delivery. *Exploration* **2024**, *4*, 20230008.

https://doi.org/10.1021/acs.jproteome.4c01046
J. Proteome Res. 2025, 24, 2771−2782

(29) Lopez-Cano, J. J.; Gonzalez-Cela-Casamayor, M. A.; Andres-Guerrero, V.; Herrero-Vanrell, R.; Benitez-Del-Castillo, J. M.; Molina-Martinez, I. T. Combined hyperosmolarity and inflammatory conditions in stressed human corneal epithelial cells and macrophages to evaluate osmoprotective agents as potential DED treatments. *Exp. Eye Res.* **2021**, *211*, 108723.
(30) Krumpochova, P.; Bruyneel, B.; Molenaar, D.; Koukou, A.; Wuhrer, M.; Niessen, W. M.; Giera, M. Amino acid analysis using chromatography-mass spectrometry: An inter platform comparison study. *J. Pharm. Biomed. Anal.* **2015**, *114*, 398−407.
(31) Berg, S.; Kutra, D.; Kroeger, T.; Straehle, C. N.; Kausler, B. X.; Haubold, C.; Schiegg, M.; Ales, J.; Beier, T.; Rudy, M.; Eren, K.; Cervantes, J. I.; Xu, B.; Beuttenmueller, F.; Wolny, A.; Zhang, C.; Koethe, U.; Hamprecht, F. A.; Kreshuk, A. ilastik: interactive machine learning for (bio)image analysis. *Nat. Methods* **2019**, *16* (12), 1226−1232.
(32) Chen, L.; Li, J.; Guo, T.; Ghosh, S.; Koh, S. K.; Tian, D.; Zhang, L.; Jia, D.; Beuerman, R. W.; Aebersold, R.; Chan, E. C.; Zhou, L. Global Metabonomic and Proteomic Analysis of Human Conjunctival Epithelial Cells (IOBA-NHC) in Response to Hyperosmotic Stress. *J. Proteome Res.* **2015**, *14* (9), 3982−3995.
(33) Mackenzie, B.; Erickson, J. D. Sodium-coupled neutral amino acid (System N/A) transporters of the SLC38 gene family. *Pfluegers Arch.* **2004**, *447* (5), 784−795.
(34) Hatanaka, T.; Huang, W.; Wang, H.; Sugawara, M.; Prasad, P. D.; Leibach, F. H.; Ganapathy, V. Primary structure, functional characteristics and tissue expression pattern of human ATA2, a subtype of amino acid transport system A. *Biochim. Biophys. Acta Biomembr.* **2000**, *1467* (1), 1−6.
(35) Hyde, R.; Cwiklinski, E. L.; MacAulay, K.; Taylor, P. M.; Hundal, H. S. Distinct Sensor Pathways in the Hierarchical Control of SNAT2, a Putative Amino Acid Transceptor, by Amino Acid Availability. *J. Biol. Chem.* **2007**, *282* (27), 19788−19798.
(36) Gaccioliy, F.; Huang, C. C.; Wang, C.; Bevilacqua, E.; Franchi-Gazzola, R.; Gazzola, G. C.; Bussolati, O.; Snider, M. D.; Hatzoglou, M. Amino Acid Starvation Induces the SNAT2 Neutral Amino Acid Transporter by a Mechanism That Involves Eukaryotic Initiation Factor 2α Phosphorylation and cap-independent Translation *. *J. Biol. Chem.* **2006**, *281* (26), 17929−17940.
(37) Hyde, R.; Christie, G. R.; Litherland, G. J.; Hajduch, E.; Taylor, P. M.; Hundal, H. S. Subcellular localization and adaptive up-regulation of the System A (SAT2) amino acid transporter in skeletal-muscle cells and adipocytes. *Biochem. J.* **2001**, *355* (3), 563−568.
(38) Hoffmann, T. M.; Cwiklinski, E.; Shah, D. S.; Stretton, C.; Hyde, R.; Taylor, P. M.; Hundal, H. S. Effects of Sodium and Amino Acid Substrate Availability upon the Expression and Stability of the SNAT2 (SLC38A2) Amino Acid Transporter. *Front. Pharmacol* **2018**, *9*, 63.
(39) Franchi-Gazzola, R.; Dall'Asta, V.; Sala, R.; Visigalli, R.; Bevilacqua, E.; Gaccioli, F.; Gazzola, G. C.; Bussolati, O. The role of the neutral amino acid transporter SNAT2 in cell volume regulation. *Acta Physiol.* **2006**, *187* (1−2), 273−283.
(40) Dall'Asta, V.; Bussolati, O.; Sala, R.; Parolari, A.; Alamanni, F.; Biglioli, P.; Gazzola, G. C. Amino acids are compatible osmolytes for volume recovery after hypertonic shrinkage in vascular endothelial cells. *Am. J. Physiol.* **1999**, *276* (4), C865−C872.
(41) Dall'Asta, V.; Rossi, P. A.; Bussolati, O.; Gazzola, G. C. Response of human fibroblasts to hypertonic stress. Cell shrinkage is counteracted by an enhanced active transport of neutral amino acids. *J. Biol. Chem.* **1994**, *269* (14), 10485−10491.
(42) Fumarola, C.; Zerbini, A.; Guidotti, G. G. Glutamine deprivation-mediated cell shrinkage induces ligand-independent CD95 receptor signaling and apoptosis. *Cell Death Differ.* **2001**, *8* (10), 1004−1013.
(43) Ouyang, W.; Yan, D.; Hu, J.; Liu, Z. Multifaceted mitochondrial as a novel therapeutic target in dry eye: insights and interventions. *Cell Death Discov.* **2024**, *10* (1), 398.
(44) Tilokani, L.; Nagashima, S.; Paupe, V.; Prudent, J. Mitochondrial dynamics: overview of molecular mechanisms. *Essays Biochem.* **2018**, *62* (3), 341−360.
(45) Burman, J. L.; Pickles, S.; Wang, C.; Sekine, S.; Vargas, J. N. S.; Zhang, Z.; Youle, A. M.; Nezich, C. L.; Wu, X.; Hammer, J. A.; Youle, R. J. Mitochondrial fission facilitates the selective mitophagy of protein aggregates. *J. Cell Biol.* **2017**, *216* (10), 3231−3247.
(46) Youle, R. J.; van der Bliek, A. M. Mitochondrial fission, fusion, and stress. *Science* **2012**, *337* (6098), 1062−1065.
(47) Zhang, W.; Li, H.; Ogando, D. G.; Li, S.; Feng, M.; Price, F. W.; Tennessen, J. M.; Bonanno, J. A. Glutaminolysis is Essential for Energy Production and Ion Transport in Human Corneal Endothelium. *EBioMedicine* **2017**, *16*, 292−301.
(48) Peyton, K. J.; Liu, X. M.; Yu, Y.; Yates, B.; Behnammanesh, G.; Durante, W. Glutaminase-1 stimulates the proliferation, migration, and survival of human endothelial cells. *Biochem. Pharmacol.* **2018**, *156*, 204−214.
(49) Chen, W.; Zhao, H.; Li, Y. Mitochondrial dynamics in health and disease: mechanisms and potential targets. *Signal Transduct. Targeted Ther.* **2023**, *8* (1), 333.
(50) Xie, L. L.; Shi, F.; Tan, Z.; Li, Y.; Bode, A. M.; Cao, Y. Mitochondrial network structure homeostasis and cell death. *Cancer Sci.* **2018**, *109* (12), 3686−3694.
(51) Nakatsukasa, M.; Sotozono, C.; Shimbo, K.; Ono, N.; Miyano, H.; Okano, A.; Hamuro, J.; Kinoshita, S. Amino Acid profiles in human tear fluids analyzed by high-performance liquid chromatography and electrospray ionization tandem mass spectrometry. *Am. J. Ophthalmol.* **2011**, *151* (5), 799−808 e1.
(52) Lu, M. J.; Pulido, J. S.; Baratz, K. H.; Qian, H.; Erie, J. C.; Shippy, S. A. Amino Acid Analysis of Human Tears in Dry vs. Normal Eyes by Capillary Electrophoresis. *Biochim. Biophys. Acta Mol. Cell Res.* **2008**, *49* (13), 5307.
(53) ChenZhuo, L.; Murube, J.; Latorre, A.; del Rio, R. M. Different concentrations of amino acids in tears of normal and human dry eyes. *Adv. Exp. Med. Biol.* **2002**, *506* (Pt A), 617−621.
(54) Cai, Y.; Tian, B.; Deng, Y.; Liu, L.; Zhang, C.; Peng, W.; Li, Q.; Zhang, T.; Han, M.; Xu, G. Glutamine Metabolism Promotes Renal Fibrosis through Regulation of Mitochondrial Energy Generation and Mitochondrial Fission. *Int. J. Biol. Sci.* **2024**, *20* (3), 987−1003.
(55) Dohl, J.; Passos, M. E. P.; Foldi, J.; Chen, Y.; Pithon-Curi, T.; Curi, R.; Gorjao, R.; Deuster, P. A.; Yu, T. Glutamine depletion disrupts mitochondrial integrity and impairs C2C12 myoblast proliferation, differentiation, and the heat-shock response. *Nutr. Res.* **2020**, *84*, 42−52.
(56) Rusciano, D.; Roszkowska, A. M.; Gagliano, C.; Pezzino, S. Free amino acids: an innovative treatment for ocular surface disease. *Eur. J. Pharmacol.* **2016**, *787*, 9−19.
(57) Aragona, P.; Rania, L.; Roszkowska, A. M.; Spinella, R.; Postorino, E.; Puzzolo, D.; Micali, A. Effects of amino acids enriched tears substitutes on the cornea of patients with dysfunctional tear syndrome. *Acta Ophthalmol.* **2013**, *91* (6), e437−e444.

https://doi.org/10.1021/acs.jproteome.4c01046
J. Proteome Res. 2025, 24, 2771−2782